

Paul F. von Herrmann, David J. Nickels, and Ajay Singh

Introduction

Trauma is the leading cause of morbidity and mortality among people younger than 45 years of age. Traumatic injury to the abdominal organs, with ensuing exsanguination, is the primary cause of death [1]. Of all abdominal traumatic injuries presenting to hospitals, blunt trauma comprises approximately 90 % and typically results from a motor vehicle collision or a fall. Penetrating trauma accounts for the remaining 10 % and is often a result of a bullet or knife injury. The evaluation of blunt or penetrating abdominal trauma can be one of the most challenging and resource-exhaustive aspects of acute trauma care.

In 1988, the American Association for the Surgery of Trauma (AAST) devised a set of organ injury scales (OISs) based on findings at surgical exploration. The OISs have now been defined by computed tomography (CT) criteria [2]. Accurate noninvasive assessment of injuries with CT is beneficial and can guide management. Since the development and application of these CT-based criteria, nonoperative management for blunt abdominal trauma has become increasingly common, particularly in hemodynamically stable patients. The accumulated evidence has demonstrated that minimally invasive management of blunt abdominal trauma, instead of laparotomy, results in

improved survival rates. Analogously, managing penetrating abdominal trauma with laparotomy results in a negative or nontherapeutic procedure in 15–25 % of cases, prompting a movement toward more conservative management algorithms [3].

Currently, multidetector computed tomography (MDCT) with intravenous contrast is the “gold standard” diagnostic imaging examination in hemodynamically stable patients who have intra-abdominal fluid by focused assessment with sonography for trauma (FAST) [4]. Many studies have reported that MDCT has high sensitivity, specificity, positive predictive value, negative predictive value, and accuracy in injuries to the liver, spleen, kidney and urinary bladder, hollow viscus, and major vascular structures [2–5].

FAST

FAST is a useful diagnostic tool when performed in the acute setting because it can demonstrate intra-abdominal fluid, a finding that suggests significant organ injury, with a sensitivity of 90–93 % [4]. FAST is often performed after the secondary assessment or during resuscitation efforts. Identification of intra-abdominal free fluid on FAST in a hemodynamically unstable patient is regarded as synonymous with hemoperitoneum, thereby directing the surgeon to consider the abdomen as the major source of blood loss and prompting emergent laparotomy instead of CT. Conversely, a positive FAST in a hemodynamically stable patient should be followed by a CT scan to determine the source of the fluid.

Shortcomings of FAST include its inability to qualitatively grade the extent of organ injury and its low (34–55 %) sensitivity for direct demonstration of blunt abdominal injury [4]. Other limiting factors include inability to demonstrate small amounts of free fluid, operator dependence, limited accuracy in the retroperitoneum, and large body habitus.

P.F. von Herrmann, MD
Department of Radiology,
University of Kentucky,
Lexington, KY, USA

D.J. Nickels, MD, MBA
Department of Radiology,
Division of Emergency Radiology,
University of Kentucky,
Lexington, KY, USA

A. Singh, MD (✉)
Department of Radiology,
Massachusetts General Hospital, Harvard Medical School,
10 Museum Way, # 524, Boston, MA 02141, USA
e-mail: asingh1@partners.org

Liver

The liver is the most frequently injured solid abdominal organ in blunt and penetrating trauma. Hepatic injury in patients who have sustained blunt trauma has been reported to occur in 1–8 % and in penetrating trauma in up to 39 % [1, 6]. However, with utilization of abdominal CT in the severely injured patient, hepatic injuries can be detected in up to 25 % of those with blunt trauma [7]. Mortality rates from blunt or penetrating liver injury have been reported to range from 2.8 to 11.7 % [6, 8].

Nonsurgical management is the preferred strategy for hemodynamically stable patients with blunt liver injury. Accurate characterization of the extent of the injury by CT assists the managing provider with specific information that can be followed and categorized by the AAST OIS criteria (Table 9.1).

Hepatic injuries detected by CT can be classified as lacerations, hematomas, active hemorrhage, and juxtahepatic venous injuries. Hepatic laceration is the most common type of parenchymal liver injury; it appears as an irregular, linear, or branching low-attenuation region on contrast-enhanced CT (CECT) (Fig. 9.1). Lacerations are further divided into superficial (<3 cm) or deep (>3 cm).

Hematomas that present in blunt liver trauma are designated as subcapsular or intraparenchymal. On CECT, a subcapsular hematoma appears as an elliptical collection of low-attenuation blood between the capsule of the liver and the enhancing liver parenchyma (Fig. 9.2). Intraparenchymal hematomas are characterized by focal low-attenuation regions with poorly defined, irregular margins in the liver parenchyma on CECT (Fig. 9.1). Active hemorrhage is diagnosed by identification of a focal high-attenuation area representing a collection of extravasated contrast. Active vascular extravasation can often be differentiated from clotted blood by measuring the CT attenuation coefficient. The attenuation of clotted blood ranges from 28 to 82 Hounsfield units (HU) (mean, 54 HU), whereas active arterial extravasation ranges from 91 to 274 HU (mean, 155 HU) [10]. Active contrast extravasation (ACE) changes its appearance over time; such a pattern can be demonstrated with multiphase vascular imaging, that is, during the arterial, portal venous, or delayed phases. On later vascular phase imaging, a region of ACE will increase in size and often pool or mix with non-contrasted blood in the adjacent hematoma.

Hepatic lacerations or hematomas that extend into a major venous structure indicate a severe injury and have been reported to require surgical management approximately 6.5 times more frequently than injuries not involving the hepatic veins or inferior vena cava (IVC) [11]. A CT finding that may indicate liver injury is periportal low attenuation paralleling the portal vein and its branches. Periportal low attenuation adjacent to a hepatic laceration may represent extension

Table 9.1 AAST organ injury scale for liver

Grade	Description
I	Hematoma: subcapsular, <10 % surface area Laceration: capsular tear, <1 cm in parenchymal depth
II	Hematoma: subcapsular, 10–50 % surface area; intraparenchymal, <10 cm in diameter Laceration: 1–3 cm in parenchymal depth, <10 cm in length
III	Hematoma: subcapsular, >50 % surface area or expanding or ruptured subcapsular parenchymal hematoma; intraparenchymal hematoma >10 cm or expanding or ruptured Laceration: >3 cm in parenchymal depth
IV	Laceration: parenchymal disruption involving 25–75 % hepatic lobe or 1–3 Couinaud segments
V	Laceration: parenchymal disruption involving >75 % of a hepatic lobe or >3 Couinaud segments within a single lobe Vascular: juxtahepatic venous injuries (i.e., central major hepatic veins or retrohepatic vena cava)
VI	Vascular: hepatic avulsion

Source: Tinkoff et al. [9]

of hemorrhage into the periportal connective tissue, although this finding is nonspecific. It can also represent distention of the periportal lymphatic vessels as can be seen after aggressive fluid resuscitation, tension pneumothorax, or pericardial tamponade [12].

Spleen

Currently, 60–80 % of patients who sustain blunt splenic injury are managed nonoperatively with a success rate near 95 % [2]. Nonoperative management of isolated splenic injury is contingent on hemodynamic stability. Inevitably, failure of nonoperative management correlates with the presence of ACE on CT scan as well as with the radiological grade of the injury per the AAST criteria [9] (Table 9.2).

CECT can accurately diagnose the four common types of splenic injury: hematoma, laceration, active hemorrhage, and vascular injuries [13]. Splenic hematomas may be classified as subcapsular or intraparenchymal. On CECT, a subcapsular hematoma appears as an elliptical, low-attenuating collection between the splenic capsule and the enhancing splenic parenchyma (Fig. 9.3). Acute lacerations have a jagged or sharp margin and appear on CECT as a linear or branching low-attenuation area.

Active hemorrhage in the spleen is represented as an irregular or linear focus of contrast extravasation on CECT. Active hemorrhage may be seen in several locations: within splenic parenchyma or subcapsular space or intraperitoneally. Differentiating between ACE (range 85–350 HU, mean 132 HU) and hematoma or clotted blood (range 40–70 HU, mean 51 HU) is accomplished by measuring the attenuation coefficient [13].

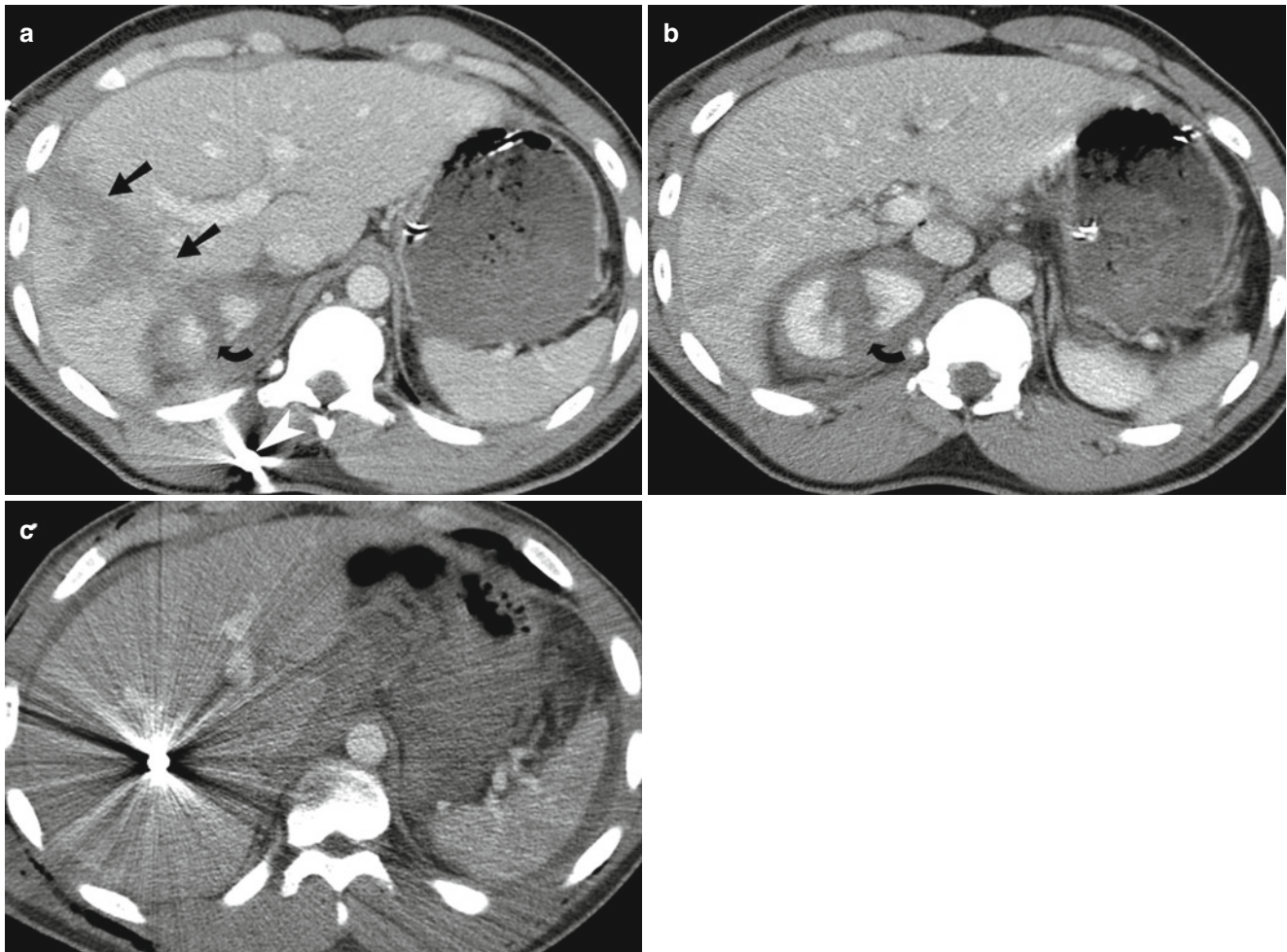


Fig. 9.1 Hepatic laceration from gunshot wound. (a and b) Contrast-enhanced CT demonstrates a deep hepatic (*straight arrow*) as well as a right renal laceration (*curved arrow*). There is a bullet fragment (*white arrowhead*) located in the right posterior abdominal wall. (c) Contrast-

enhanced CT demonstrates a metallic density bullet fragment located centrally within the right lobe of liver. The liver laceration is obscured by the extensive beam-hardening artifact produced by the bullet fragment

Splenic vascular injuries include post-traumatic pseudoaneurysms and arteriovenous (AV) fistulas. A splenic pseudoaneurysm will appear as a well-circumscribed focus of increased attenuation in comparison to the enhancing splenic parenchyma (Fig. 9.4). An AV fistula is best demonstrated by early splenic vein enhancement. Both of these vascular injuries are best seen on arterial phase imaging and can be difficult to detect on portal venous phase or delayed (renal excretory phase) imaging. If a splenic pseudoaneurysm is suspected on early arterial phase imaging, it is helpful to distinguish this finding from ACE by noting the characteristics on delayed imaging. Specifically, on delayed imaging, a pseudoaneurysm will remain the same size and demonstrate similar density to the aorta, but ACE will increase in size and remain with high density. Splenic vascular lesions can be managed successfully by splenic arteriographic embolization, which improves the success rate of nonoperative management of blunt splenic injuries from 87 to 94 % [14, 15].

Pancreas

Pancreatic injuries have been reported as high as 12 % in victims of blunt trauma and 6 % in those with penetrating trauma. Typically, pancreatic injuries are associated with other intra-abdominal injuries 50–98 % of the time [13]. The clinical diagnosis of pancreatic injury may be difficult, particularly when isolated. Owing to the retroperitoneal location of the pancreas, peritonitis from a pancreatic injury may take hours to days to manifest. In addition, serum and urinary amylase levels are unreliable markers for the diagnosis of pancreatic injury [16].

CECT is the modality of choice for diagnosing pancreatic injury; its reported sensitivity and specificity is as high as 85 % [17]. CECT findings of pancreatic injury may be subtle, and the pancreas may appear normal immediately post-injury. Of primary importance is evaluation of the pancreatic duct because its integrity or lack of integrity directs management.

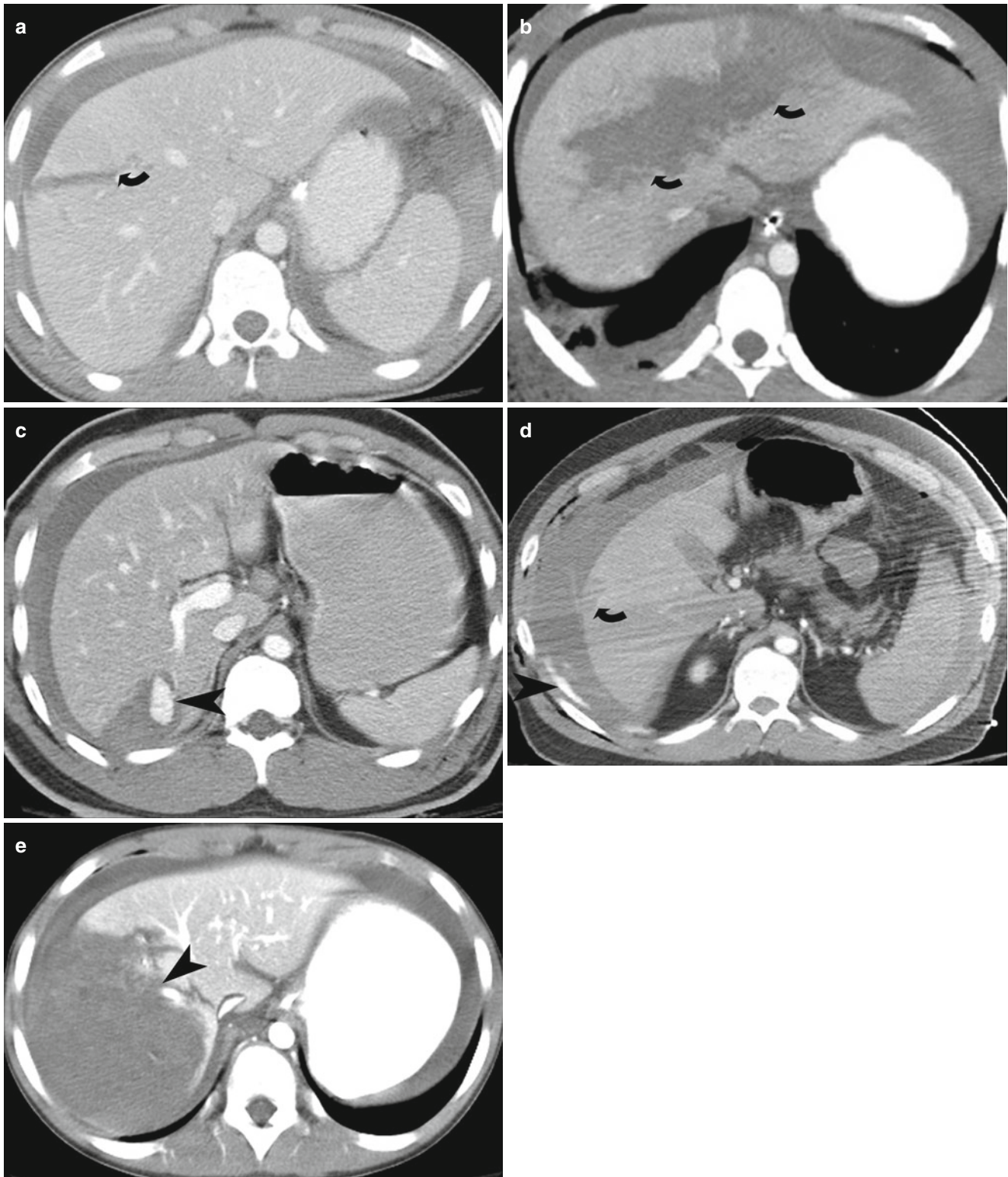


Fig. 9.2 Hepatic lacerations. (a and b) Contrast-enhanced CT in two different patients show a deep (>3 cm) hepatic laceration (grade III and grade IV liver injury) (*curved arrows*) due to stab injury. (c) Contrast-enhanced CT shows a wedge shaped liver laceration due to stab injury with subcapsular hematoma and enhancing pseudoaneurysm (*arrowhead*).

(d) Contrast-enhanced CT shows a large perihepatic hematoma and active extravasation (*arrowhead*) arising from a gunshot injury related superficial liver laceration (*curved arrow*). (e) Contrast-enhanced CT shows grade IV liver injury with devascularization of >25 % of the right lobe of the liver (*arrowhead*)

Table 9.2 AAST organ injury scale for spleen

Grade	Description
I	Hematoma: subcapsular, <10 % surface area Laceration: capsular tear, <1 cm in parenchymal depth
II	Hematoma: subcapsular, 10–50 % surface area; intraparenchymal, <5 cm in diameter Laceration: capsular tear, 1–3 cm in parenchymal depth, not involving a trabecular vessel
III	Hematoma: subcapsular, >50 % surface area or expanding; ruptured subcapsular or parenchymal hematoma; intraparenchymal hematoma >5 cm or expanding Laceration: >3 cm in parenchymal depth or involving trabecular vessels
IV	Laceration: involving segmental or hilar vessels producing major devascularization (>25 % of spleen)
V	Hematoma: completely shattered spleen Laceration: hilar vascular injury that devascularizes spleen

Source: Tinkoff et al. [9]

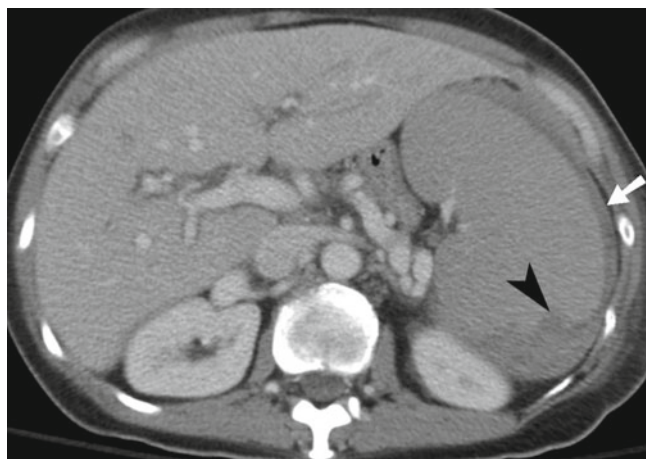


Fig. 9.3 Splenic laceration. Contrast-enhanced CT shows subcapsular hematoma (*arrow*) and intraparenchymal laceration (*arrowhead*) with hematoma

A pancreatic injury can be categorized as contusion, laceration, or transection. A pancreatic contusion may appear as diffuse enlargement of the pancreas or as focal low attenuation or heterogeneity. Pancreatic lacerations are demonstrated by linear, irregular low-attenuation areas within the normally enhancing parenchyma (Fig. 9.5). A pancreatic transection may be difficult to diagnose with CT unless there is low-attenuation fluid collection separating the two edges of the transected pancreas.

The position of the pancreatic laceration in relation to the superior mesenteric artery as well as the depth of the laceration helps predict pancreatic ductal disruption, which occurs in up to 15 % of pancreatic trauma [13, 17]. The superior mesenteric vessels provide a landmark for dividing the pancreas into proximal and distal portions with injury to the

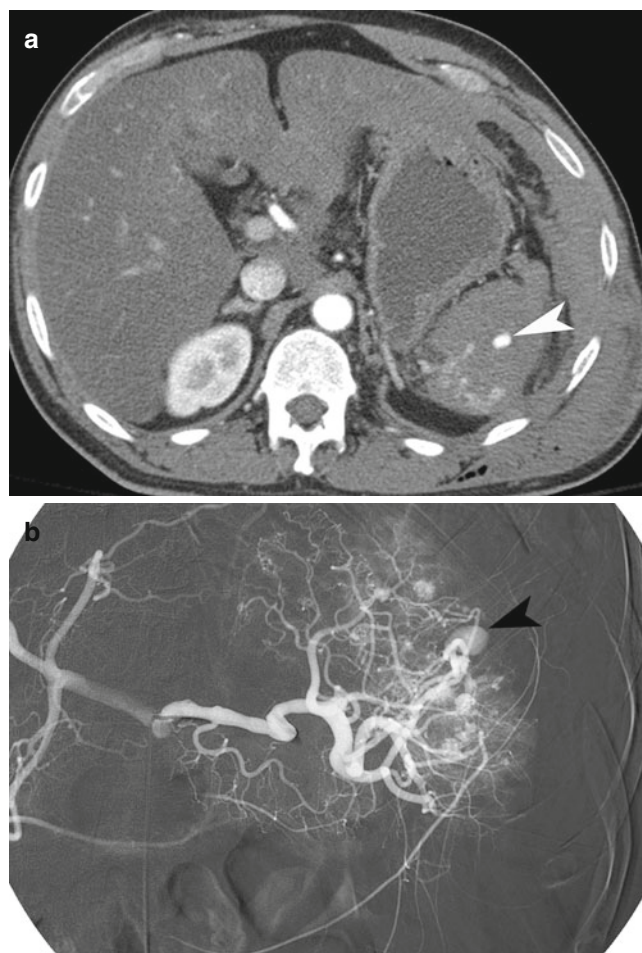


Fig. 9.4 Splenic pseudoaneurysm. (a) Contrast-enhanced CT demonstrates a pseudoaneurysm (*arrowhead*) within the splenic parenchymal laceration. (b) Conventional splenic artery angiogram demonstrates the splenic arterial branch pseudoaneurysm (*arrowhead*)

proximal pancreas usually associated with more severe injury. A laceration of the pancreas involving >50 % of the anteroposterior diameter of the pancreatic body or tail is often associated with ductal disruption.

There are several nonspecific CT findings associated with pancreatic trauma, the most common of which is thickening or infiltration of the anterior pararenal fascia. Additional nonspecific CT findings include blood/fluid tracking along the mesenteric vessels, fluid in the lesser sac, fluid between the pancreas and splenic vein, or infiltration of the peripancreatic fat with fluid or hemorrhage [13].

Kidney

The kidney is the most commonly injured urogenital organ in trauma. Approximately 10 % of all significant blunt abdominal traumatic injuries include a renal injury, and of those, 80–90 % are managed nonoperatively. The goal of

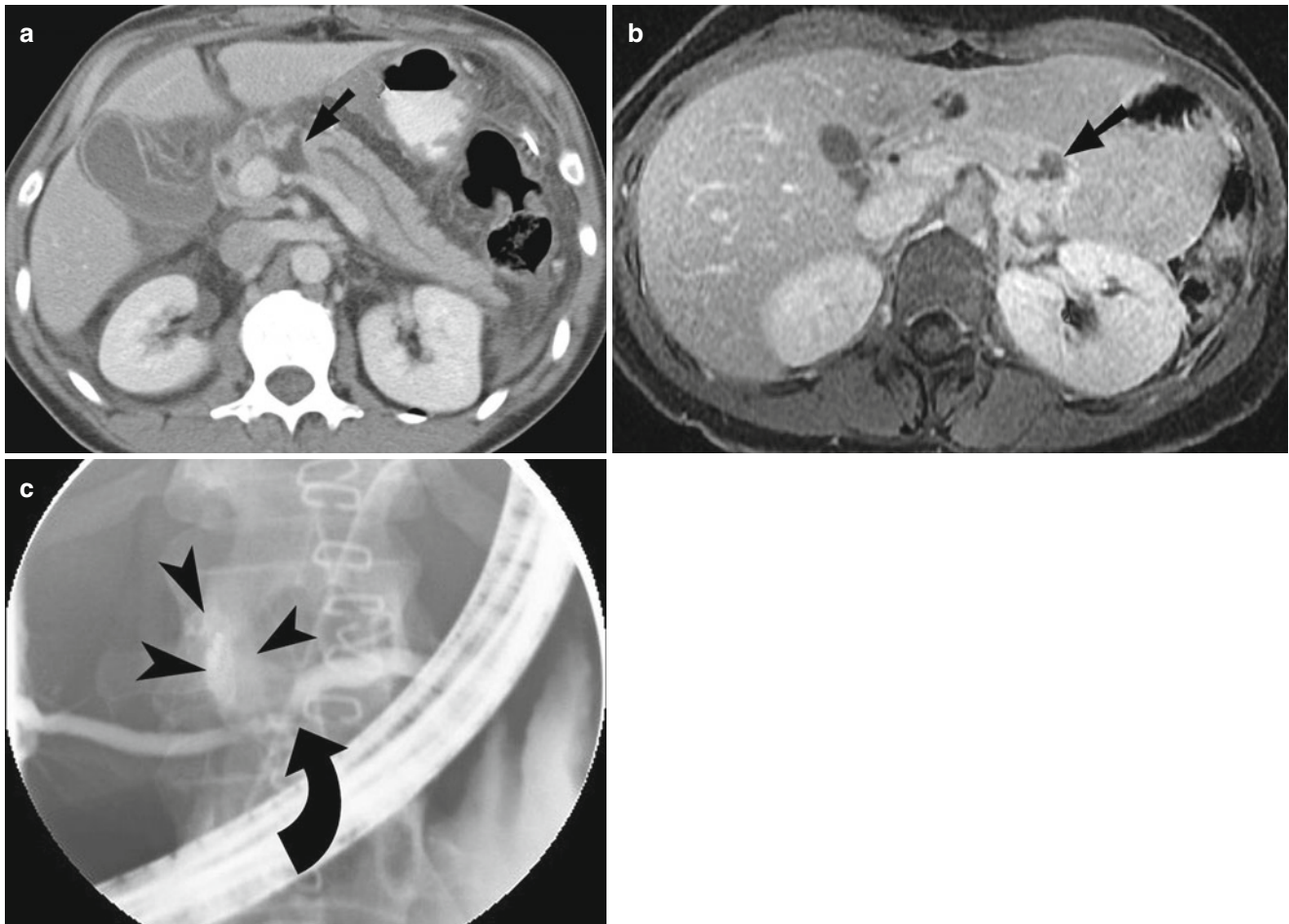


Fig. 9.5 Pancreatic injury. (a and b) Contrast-enhanced CT demonstrates pancreatic laceration (*arrow*) with disruption of the main pancreatic duct. (c) Endoscopic retrograde cholangiopancreatography

image showing pancreatic duct discontinuity (*curved arrow*) and extravasation of contrast from the ductal disruption (*arrowheads*)

conservative management is to preserve organ integrity and reduce the complication rate. Historical evidence shows that hemodynamically stable patients with kidney injuries who undergo surgical exploration have a much higher incidence of nephrectomy [4]. Blunt trauma accounts for approximately 90 % of renal trauma, while penetrating trauma accounts for approximately 10 %. Nonsurgical management is more commonly advocated in blunt renal injuries, but conservative protocols have also been applied to penetrating renal injuries [18, 19]. However, penetrating trauma is more frequently associated with major renal injury and frequently requires invasive treatment, as it is more often associated with hemodynamic instability and damage to surrounding abdominal organs [20]. Indications for renal imaging include gross hematuria and penetrating or blunt trauma with hematuria. The imaging modality of choice to evaluate the kidneys after trauma is CECT.

Renal injuries may be classified as lacerations, contusions, or renovascular injuries, which determine the radiological grade of the injury per AAST criteria (Table 9.3).

Renal contusions are visualized as poorly margined, round or ovoid areas of low-attenuation and show a delayed or persistent nephrogram when compared to normal adjacent renal parenchyma. Hematomas can be categorized as subcapsular or perinephric. On an unenhanced CT, a subcapsular hematoma (Fig. 9.6) is seen as an eccentric hyperattenuating fluid collection confined between the renal parenchyma and renal capsule. However, on a CECT a subcapsular hematoma will be hypoattenuating compared to the normal enhancing renal parenchyma. A subcapsular hematoma may also exert a mass effect on the renal contour and can cause decreased perfusion in extreme cases. A perinephric hematoma is a poorly margined, hyperattenuating fluid collection (45–90 HU) that is confined between the renal parenchyma and the Gerota fascia [21]. Other findings associated with a perinephric hematoma are thickening of the lateroconal fascia, compression of the colon, and displacement of the kidney.

Renal lacerations are visualized as hypoattenuating, irregular wedge-shaped, or linear parenchymal defects or clefts (Figs. 9.7 and 9.8). The most severe form of renal laceration,

Table 9.3 AAST organ injury scale for kidney

Grade	Description
I	Hematoma: subcapsular, nonexpanding without parenchymal laceration Contusion: microscopic or gross hematuria, urologic studies normal
II	Hematoma: nonexpanding perirenal hematoma confirmed to renal retroperitoneum Laceration: <1 cm parenchymal depth of renal cortex without urinary extravasation
III	Laceration: >1 cm in parenchymal depth of renal cortex without collecting system rupture or urinary extravasation
IV	Laceration: parenchymal laceration extending through renal cortex, medulla, and collecting system Vascular: main renal artery or vein injury with contained hemorrhage
V	Hematoma: completely shattered kidney Vascular: avulsion of renal hilum that devascularizes kidney

Source: Tinkoff et al. [9]

termed a “shattered kidney,” represents a kidney that is fractured into multiple fragments. It is often associated with devitalized renal tissue, injuries to the collecting system, severe hemorrhage, active arterial bleeding, and compromise in the excretion of contrast material [21].

The depth of a renal laceration is important as it relates to the renal collecting system. If a laceration extends into the collecting system, this is consistent with a higher-grade injury (IV or V instead of III). Renal pelvis or collecting system involvement can be demonstrated by urine extravasation, which is seen as a perinephric low-density fluid collection on arterial or portal venous phase imaging. Suspected urine extravasation can be differentiated from hematoma by the presence of contrast extravasation, which is only seen on the delayed renal excretory phase images.

Urinary Bladder

Bladder injuries are caused by blunt or penetrating trauma. Blunt trauma accounts for 60–85 % of bladder injuries, whereas penetrating trauma accounts for 15–40 % [22]. The conventional mechanism of injury to the bladder in blunt abdominal trauma is rapid increase of the intravesical pressure resulting in a tear along the intraperitoneal portion of the bladder wall. Bladder injury is more common among those sustaining a seatbelt or steering wheel injury.

Bladder rupture should be suspected when a patient presents with gross hematuria, pelvic fluid, and/or pelvic fractures. Certain types of pelvic fractures are associated with bladder rupture; these include sacral, iliac, and pubic rami fractures as well as pubic symphysis diastasis and sacroiliac joint



Fig. 9.6 Page kidney. (a and b) Axial and coronal contrast-enhanced CT images demonstrate subcapsular hematoma (arrowhead) compressing the left renal cortex

diastasis [23]. In patients with pelvic fractures, bladder injury occurs in approximately 10 %; however, traumatic extraperitoneal ruptures of the bladder are predominantly associated with pelvic fractures [24]. CT cystography or conventional fluoroscopic cystography should be performed following CT of the abdomen and pelvis in hemodynamically stable trauma patients with (1) gross hematuria, (2) pelvic fracture (other than an isolated acetabular fracture) plus microhematuria (>25 RBC/HPC), or (3) microhematuria and pelvic fluid.

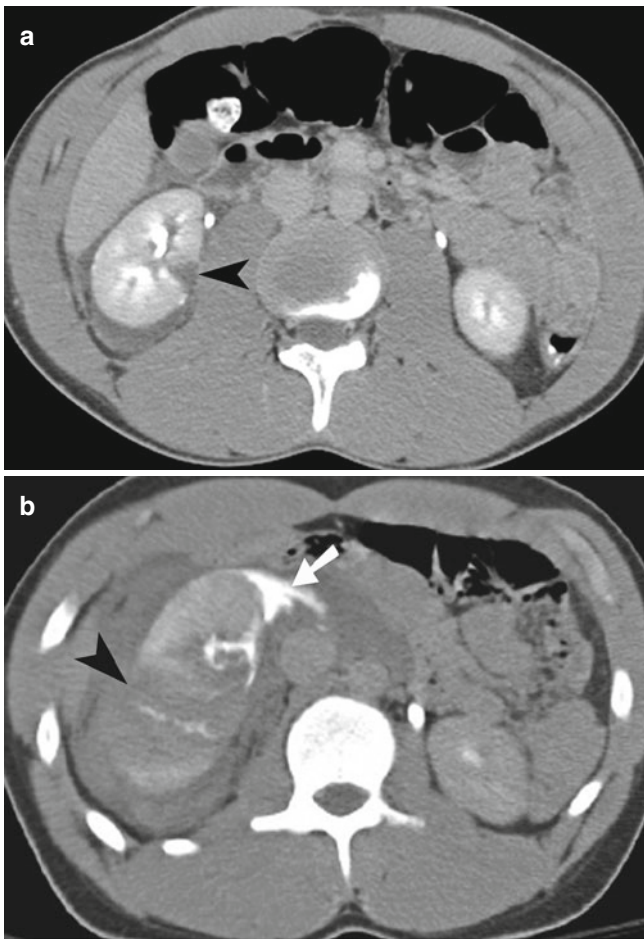


Fig. 9.7 Renal laceration. (a) Axial contrast-enhanced CT demonstrating a grade II laceration (*arrowhead*) with small perinephric hematoma. (b) Axial contrast-enhanced CT demonstrates grade V shattered kidney (*arrowhead*) and extravasation of urine (*white arrow*) into the perinephric space

CT cystography has a similar sensitivity and specificity to conventional fluoroscopic cystography and provides a more complete and more sensitive evaluation of the urinary bladder than a conventional abdominal and pelvic CT [25].

On abdominal CT, findings suggestive of urinary bladder injury or rupture include the presence of free fluid in the pelvis with no obvious source, urinary contrast extravasation, bladder wall discontinuity, and the presence of any foreign body within the bladder wall (Figs. 9.9, 9.10, and 9.11). On CT cystography, extraperitoneal injuries can be distinguished from intraperitoneal injuries by the location of the extravasation in relation to the peritoneal reflection. An extraperitoneal injury is below the peritoneal reflection and will demonstrate contrast extravasation in the classic “flame-shaped” or “molar tooth” configuration as the contrast penetrates into the paravesical tissues. In the case of intraperitoneal bladder injuries, the perforation is above the peritoneal reflection and extravasated contrast will outline bowel loops. Injuries to the neck of the bladder will show

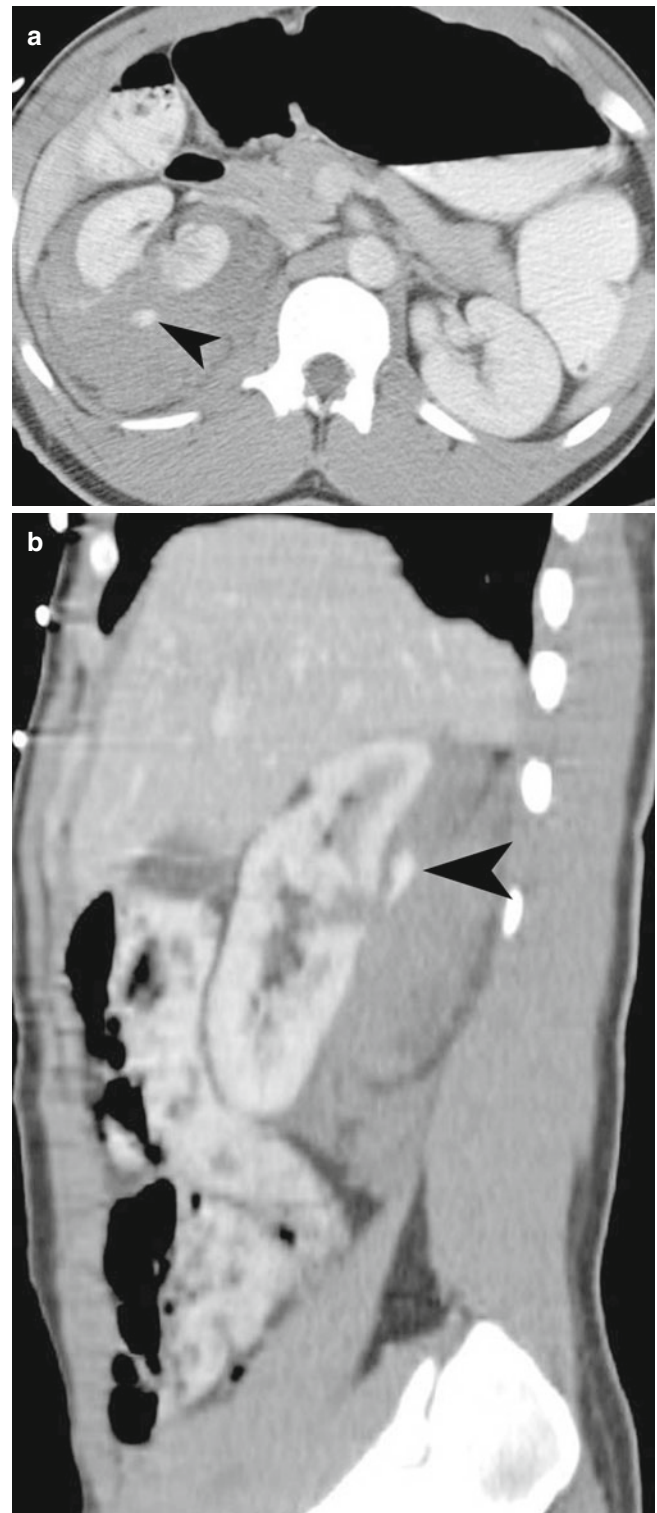


Fig. 9.8 Renal injury, CECT. (a and b) Axial and sagittal contrast-enhanced CT demonstrate right renal laceration with extravasation of contrast (*arrowhead*) into a perinephric hematoma

extravasation near the base of the bladder. The pattern of contrast extravasation on cystography is of foremost importance and will guide management of the patient.

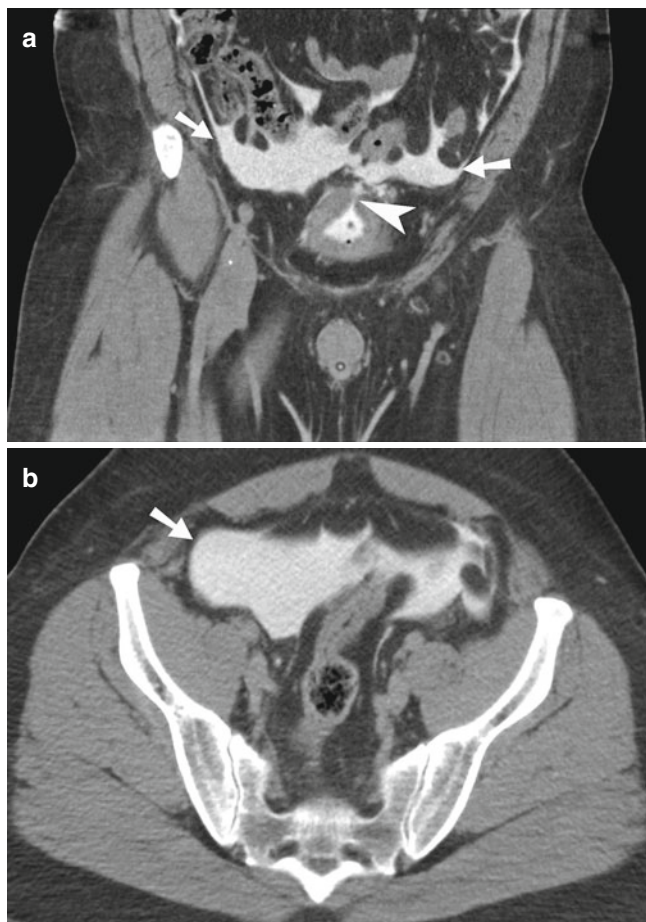


Fig. 9.9 Intraperitoneal bladder rupture. (a and b) Coronal CT cystogram image demonstrating large amount of intraperitoneal contrast (arrows) leaking from the dome of the urinary bladder (arrowhead) and outlining the small bowel loops

Urethra

Injuries to the urethra are most often caused by a displaced anterior arch pelvic fracture or iatrogenic manipulation [26]. Approximately 10–25 % of patients with a pelvic fracture also have urethral trauma. Urethral injury is most often diagnosed with a retrograde urethrogram (RUG), which should be performed prior to insertion of a urethral catheter to avoid further injury. The ultimate goal of an RUG following trauma is to evaluate the integrity of the urethra and to determine if the urethra is “watertight.” Contrast extravasation during an RUG is diagnostic for urethral injury (Fig. 9.12). An RUG can also demonstrate strictures, which can be long-term sequelae of urethral injury.

Urethral injuries are divided into two categories based on the anatomical site of the injury. Posterior urethral injuries are located in the membranous and prostatic urethra. Anterior urethral injuries are located distal to the membranous urethra. Typically, both posterior and anterior urethral injuries

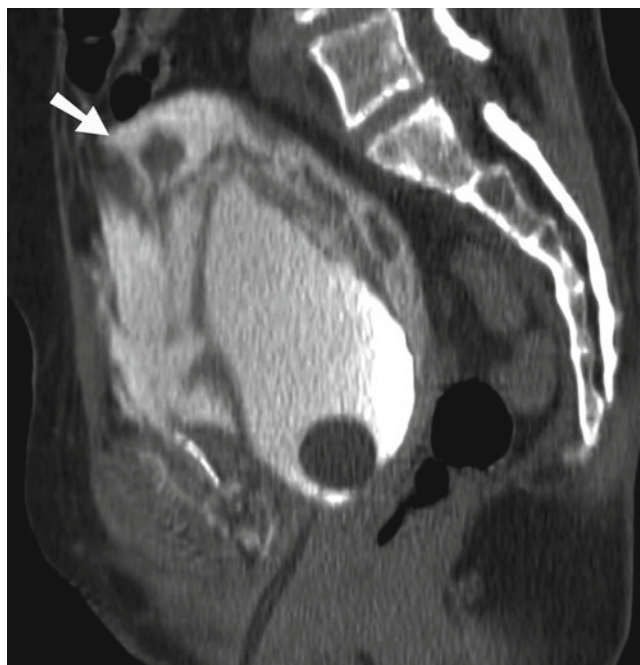


Fig. 9.10 Intraperitoneal rupture of the urinary bladder. Sagittal CT cystogram image demonstrating intraperitoneal contrast (arrow) outlining the pelvis

are the result of blunt trauma. Penetrating trauma, which includes gunshot and stab wounds, most often affects the penile urethra (Fig. 9.13).

Radiologists employ two different classification systems for grading urethral injuries. The Goldman classification (Table 9.4) is most commonly used by urologists and includes urethral injuries as well as bladder injuries that simulate posterior urethral injury. The second classification system is the AAST Organ Injury Scale for urethral injuries (Table 9.5). Imaging of the urethra with an RUG is the reference standard for urethral injury; however, with the widespread use of CT, it is vital to be familiar with CT findings indicative of urethral injury. These findings include indistinct urogenital diaphragmatic fat plane, indistinct prostatic contour, hematoma of the ischiocavernosus and obturator internus muscles, and obscuration of the bulbocavernosus muscle [27–29].

Bowel and Mesentery

Unidentified bowel and mesenteric injuries carry significant morbidity and mortality secondary to complications arising from peritonitis. Injuries to the bowel and mesentery occur in approximately 5 % of patients sustaining blunt abdominal trauma and 30 % in patients sustaining penetrating trauma to the abdomen [2, 6, 13]. Similar to pancreatic injury, the initial physical examination on a patient with mesenteric injury may be misleadingly normal. Classic peritoneal signs may be present in only one-third of patients [30].

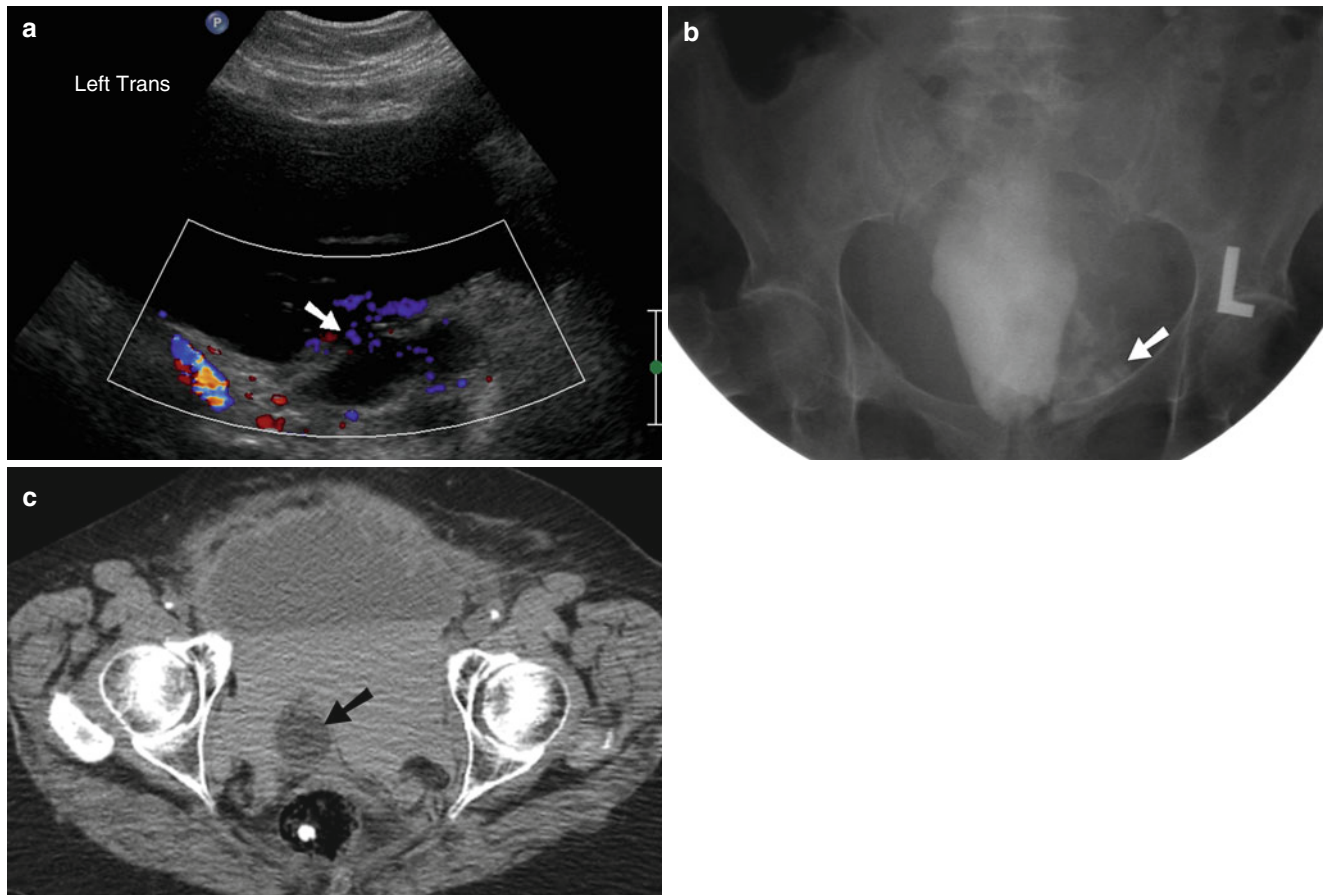


Fig. 9.11 Urinary bladder rupture. (a) Ultrasound image of the pelvis demonstrating direct transperitoneal communication (*arrow*) between urinary bladder and a large pelvic urinoma. (b) Cystogram study depicts

extravasation of contrast from the urinary bladder into the extraperitoneal space (*arrow*). (c) CT cystogram demonstrating Foley catheter bulb (*arrow*) located outside the urinary bladder in a large pelvic fluid collection

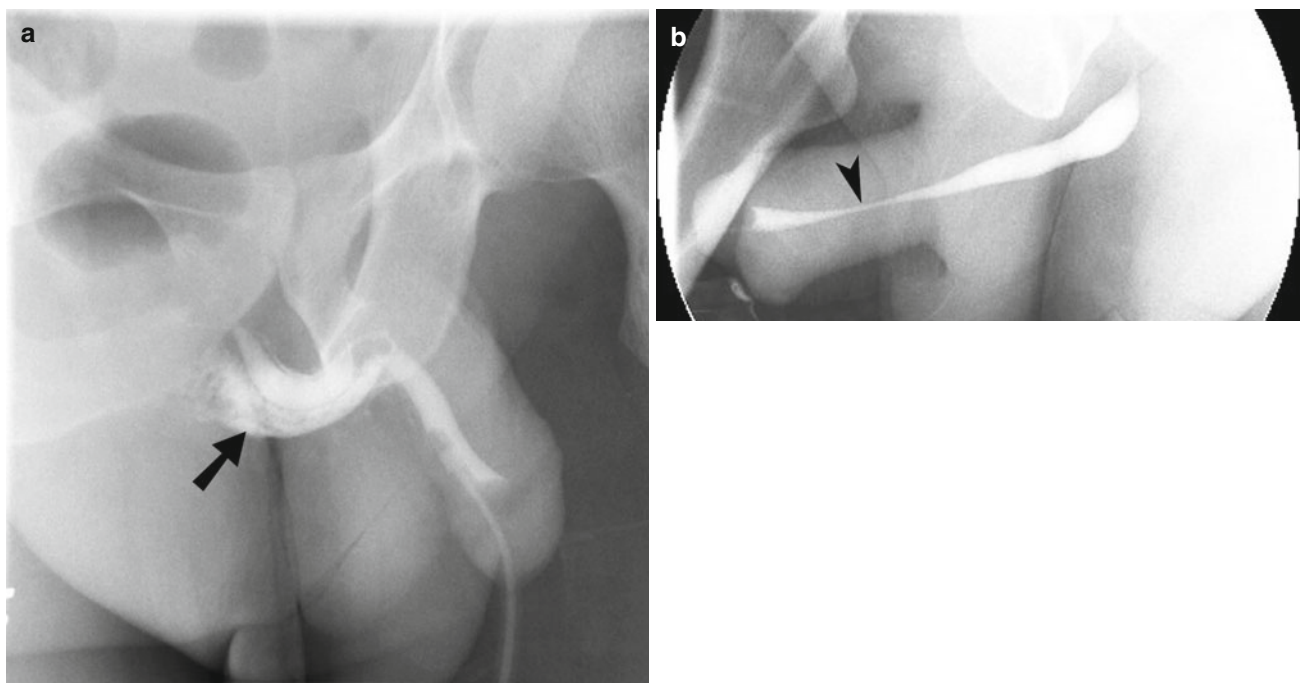


Fig. 9.12 Urethral injuries by RUG. (a) RUG demonstrating extravasation of contrast (*arrow*) from the bulbous urethra. (b) RUG demonstrating urethral narrowing (*arrowhead*) due to extrinsic compression from a penile shaft hematoma

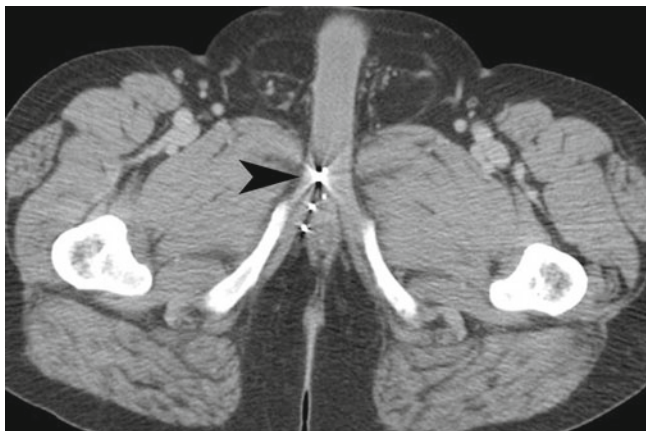


Fig. 9.13 Penile and urethral injury from shotgun pellets. Contrast-enhanced CT demonstrates multiple metallic foreign bodies (*arrowheads*) in the corpora cavernosa and spongiosum of the penis

Table 9.4 Goldman classification for urethral injuries

Grade	Description
I	Posterior urethra intact but stretched and elongated. Prostate and bladder apex displaced superiorly
II	Urethra disrupted above urogenital diaphragm in prostatic segment. Membranous urethra intact
III	Membranous urethra disrupted. Extension of injury to the proximal bulbous urethra and/or disruption of urogenital diaphragm
IV	Bladder neck injury with extension into the proximal urethra
IVA	Injury at the base of the bladder with periurethral extravasation simulating a type IV urethral injury
V	Partial or complete pure anterior urethral injury

Source: Ali et al. [27]

Table 9.5 AAST organ injury scale for urethra

Grade	Injury type	Description
I	Contusion	Blood at urethral meatus, urethrography normal
II	Stretch injury	Elongation of urethra without extravasation on urethrography
III	Partial disruption	Extravasation of urethrography contrast at injury site. Contrast visualized in bladder
IV	Complete disruption	Extravasation of urethrography contrast at injury site without contrast in bladder <2 cm of urethral separation
V	Complete disruption	Complete transection with >2 cm of urethral separation or extension into the prostate or vagina

Source: Ingram et al. [28]

Injury to the bowel and mesentery is most often diagnosed with CECT. However, there is no single CT sign that is considered both sensitive and specific for bowel or mesenteric injury. CT findings suggestive of a mesenteric injury include ACE into the mesentery, focal mesenteric hematoma or infiltration (Fig. 9.14), bowel wall thickening, or abnormal

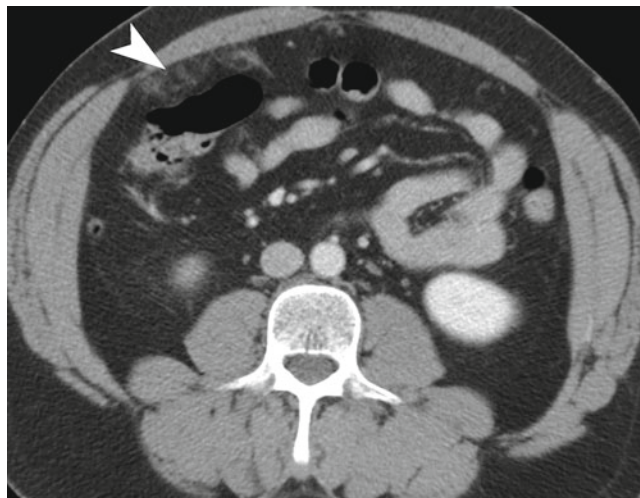


Fig. 9.14 Omental contusion. Contrast-enhanced CT demonstrates fat stranding in omental fat (*arrowhead*) due to traumatic omental contusion



Fig. 9.15 Small bowel perforation. Contrast-enhanced CT shows extravasation of oral contrast (*arrowhead*) secondary to small bowel perforation caused by trocar during laparoscopic surgery

enhancement with mesenteric hematoma. In the presence of bowel perforation (Fig. 9.15), CT findings may include extraluminal air or oral contrast (if administered), or moderate to large volumes of free intraperitoneal fluid without an obvious source such as solid organ injury [5].

Shock bowel or diffuse small bowel ischemia (Figs. 9.16 and 9.17) can occur when a patient becomes severely hypotensive following hemorrhage. Shock develops from decreased circulating blood volume, which is often complicated by derangement of circulatory control and release of vasoconstrictors such as angiotensin II, adrenaline, and norepinephrine. The blood supply to the intestinal mucosa is drastically reduced during marked sympathetic stimulation and is diverted to other crucial organs such as the brain and heart.

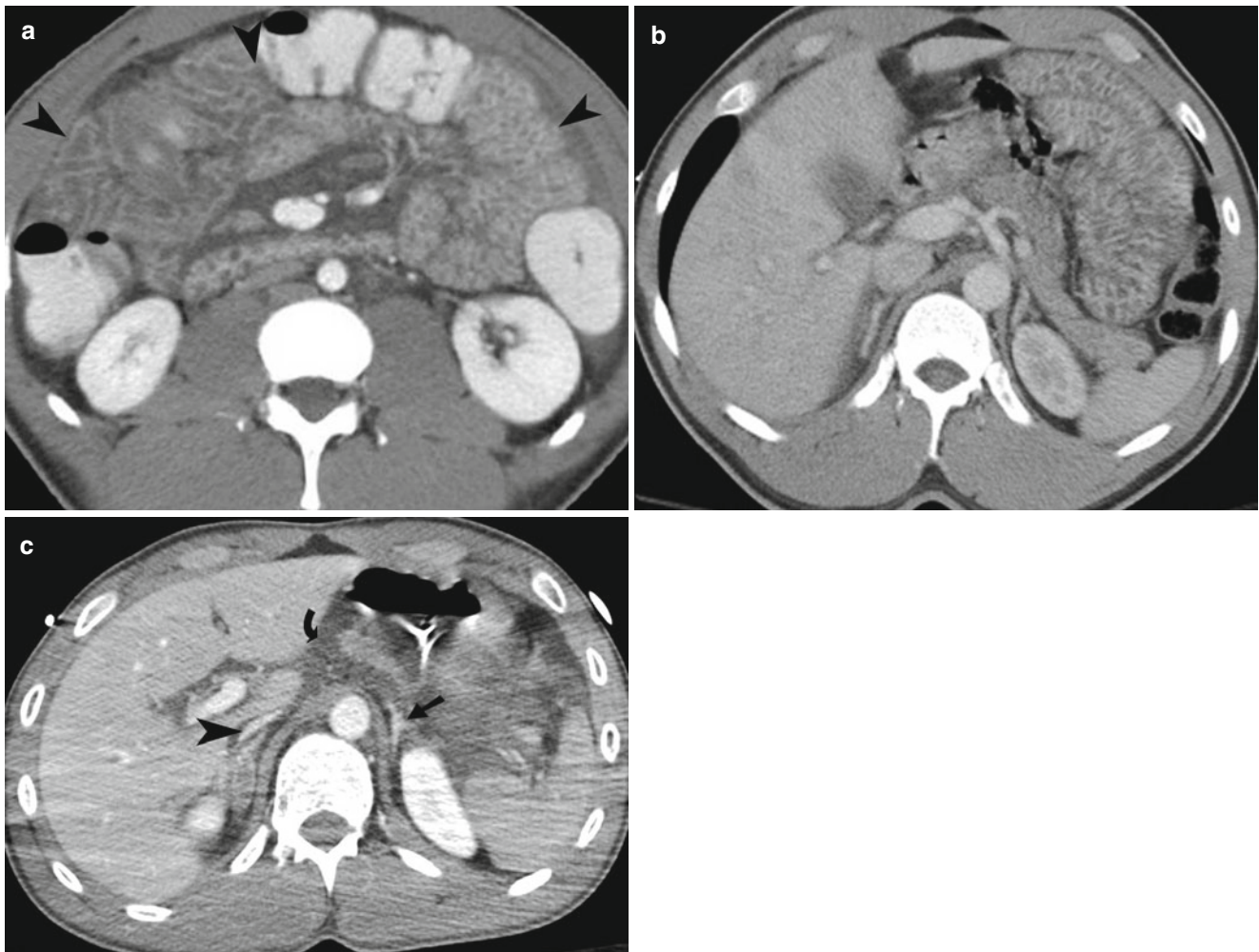


Fig. 9.16 Shock bowel syndrome. (a and b) Contrast-enhanced CT shows hyperenhancing small bowel walls (*arrowheads*) in a patient with hypovolemia after motor vehicle accident. (c) Contrast-enhanced

CT shows hyperenhancing adrenal gland (*straight arrow*), flattened IVC (*arrowhead*), and peripancreatic fluid (*curved arrow*)

The resulting splanchnic vasoconstriction leads to intestinal hypoperfusion and, in advanced cases, intestinal ischemia. Mesenteric arterial vasoconstriction and venous constriction of the bowel wall develop after release of angiotensin II, adrenaline, and noradrenaline. The resultant decrease in both arterial perfusion and venous outflow contributes to the enhancement of the bowel mucosa in shock bowel [31]. Bowel hypoperfusion most profoundly affects the intestinal mucosa, which can lead to “third space” fluid loss into the gastrointestinal tract. CT characteristics of shock bowel are diffuse thickening of the small bowel wall (7–15 mm), fluid-filled dilated small bowel, increased contrast enhancement of the small bowel wall, and flattened vena cava. The large bowel will often appear normal in the setting of small bowel ischemia.

In addition to the aforementioned effects of the hypoperfusion complex on the bowel and mesentery, shock adrenal glands play a role in the increased sympathetic stimulation

and demonstrate symmetric hyperenhancement on CT. Hypoperfusion results in the release of angiotensin II which stimulates the adrenal cortex of the adrenal glands to produce aldosterone and the adrenal medulla to produce adrenaline and noradrenaline.

Teaching Points

- Findings suggestive of mesenteric injury include ACE into the mesentery, focal mesenteric hematoma or infiltration, bowel wall thickening, or abnormal enhancement with mesenteric hematoma.
- RUG is the study of choice for the diagnosis of urethral injury.
- CT cystography or conventional cystography should be performed following abdomen/pelvis CT if bladder injury is suspected.

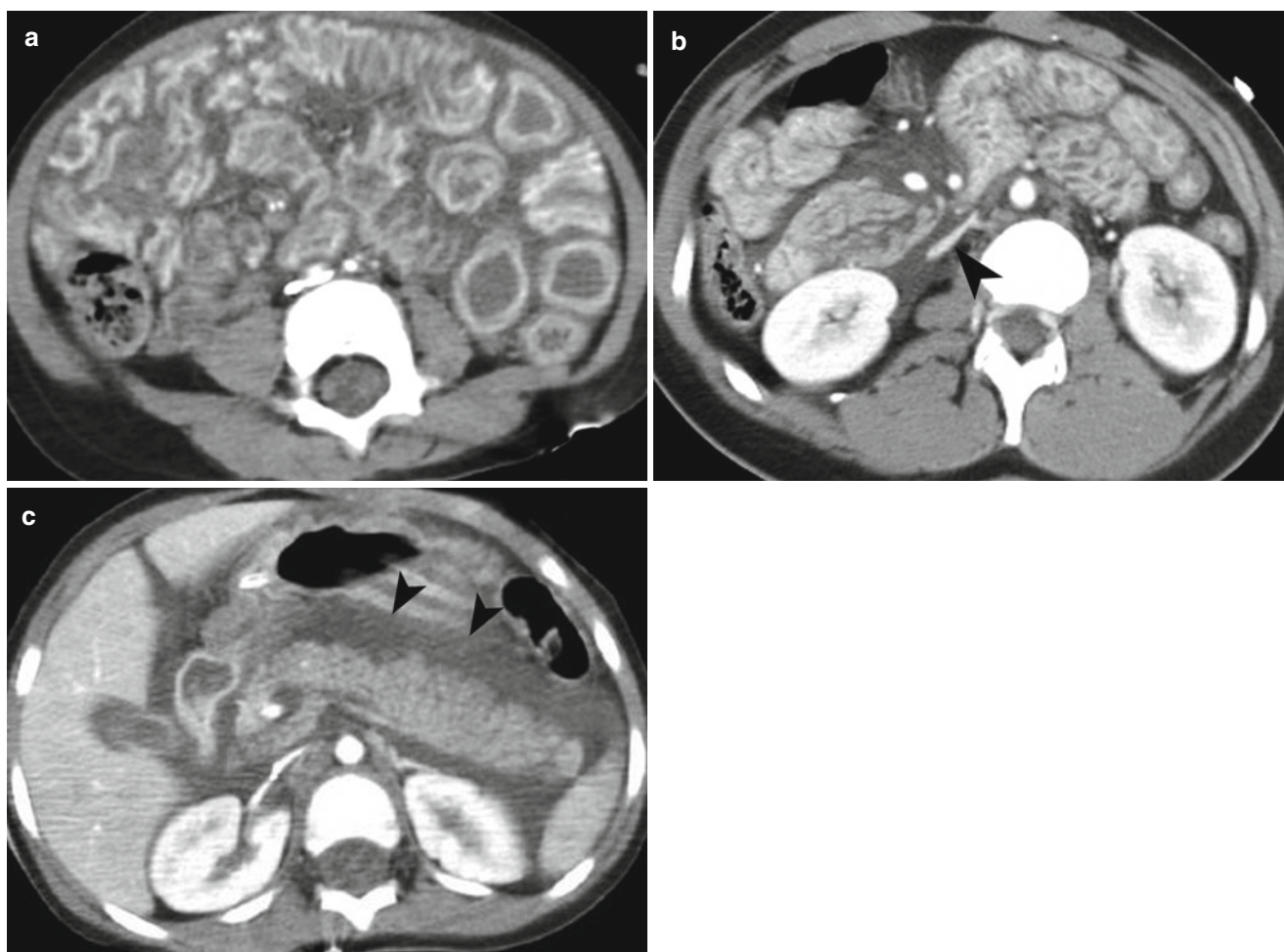


Fig. 9.17 Shock bowel syndrome. (a and b) Contrast-enhanced CT shows hyperenhancing small bowel walls and ascites. The IVC (arrowhead) is flattened secondary to hypovolemia. (c) Contrast-enhanced CT shows peripancreatic fluid (arrowheads) and flattened IVC

- Bowel perforation may show extraluminal air or oral contrast, or moderate to large volume of intraperitoneal free fluid without an obvious source.
- Shock bowel appears as diffuse thickening of the small bowel wall (7–15 mm), fluid-filled dilated small bowel, increased contrast enhancement of the small bowel wall, and flattened vena cava.

References

1. Sauaia A, Moore FA, Moore EE, Moser KS, Brennan R, Read RA, et al. Epidemiology of trauma deaths: a reassessment. *J Trauma*. 1995;38:185–93.
2. Milia DJ, Brasel K. Current use of CT in the evaluation and management of injured patients. *Surg Clin North Am*. 2011;91:233–48.
3. Melo EL, de Menezes MR, Cerri GG. Abdominal gunshot wounds: multi-detector-row CT findings compared with laparotomy—a prospective study. *Emerg Radiol*. 2012;19:35–41.
4. van der Vlies CH, Olthof DC, Gaakeer M, Ponsen KJ, van Delden OM, Goslings JC. Changing patterns in diagnostic strategies and the treatment of blunt injury to solid abdominal organs. *Int J Emerg Med*. 2011;4:47.
5. Butela ST, Federle MP, Chang PJ, Thaete FL, Peterson MS, Dorvauld CJ, et al. Performance of CT in detection of bowel injury. *AJR Am J Roentgenol*. 2001;176:129–35.
6. Feliciano DV, Rozycki GS. The management of penetrating abdominal trauma. *Adv Surg*. 1995;28:1–39.
7. Matthes G, Stengel D, Seifert J, Rademacher G, Mutze S, Ekkernkamp A. Blunt liver injuries in polytrauma: results from a cohort study with the regular use of whole-body helical computed tomography. *World J Surg*. 2003;27:1124–30.
8. Yoon W, Jeong YY, Kim JK, Seo JJ, Lim HS, Shin SS, et al. CT in blunt liver trauma. *Radiographics*. 2005;25:87–104.
9. Tinkoff G, Esposito TJ, Reed J, Kilgo P, Fildes J, Pasquale M, et al. American association for the surgery of trauma organ injury scale: spleen, liver, and kidney, validation based on the national trauma data bank. *J Am Coll Surg*. 2008;207:646–55.
10. Willmann JK, Roos JE, Platz A, Pfammatter T, Hilfiker PR, Marincek B, et al. Multidetector CT: detection of active hemorrhage in patients with blunt abdominal trauma. *AJR Am J Roentgenol*. 2002;179:437–44.
11. Poletti PA, Mirvis SE, Shanmuganathan K, Killeen KL, Coldwell D. CT criteria for management of blunt liver trauma: correlation with angiographic and surgical findings. *Radiology*. 2000;216:418–27.

12. Shanmuganathan K, Mirvis SE. CT scan evaluation of blunt hepatic trauma. *Radiol Clin North Am.* 1998;36:399–411.
13. Shanmuganathan K. Multi-detector row CT imaging of blunt abdominal trauma. *Semin Ultrasound CT MR.* 2004;25:180–204.
14. Davis KA, Fabian TC, Croce MA, Gavant ML, Flick PA, Minard G, et al. Improved success in nonoperative management of blunt splenic injuries: embolization of splenic artery pseudoaneurysms. *J Trauma.* 1998;44:1008–13; discussion 1013–5.
15. Shanmuganathan K, Mirvis SE, Boyd-Kranis R, Takada T, Scalea TM. Nonsurgical management of blunt splenic injury: use of CT criteria to select patients for splenic arteriography and potential endovascular therapy. *Radiology.* 2000;217:75–82.
16. Craig MH, Talton DS, Hauser CJ, Poole GV. Pancreatic injuries from blunt trauma. *Am Surg.* 1995;61:125–8.
17. Fisher M, Brasel K. Evolving management of pancreatic injury. *Curr Opin Crit Care.* 2011;17:613–7.
18. Broghammer JA, Fisher MB, Santucci RA. Conservative management of renal trauma: a review. *Urology.* 2007;70:623–9.
19. Meng MV, Brandes SB, McAninch JW. Renal trauma: indications and techniques for surgical exploration. *World J Urol.* 1999;17:71–7.
20. Sica G, Bocchini G, Guida F, Tanga M, Guaglione M, Scaglione M. Multidetector computed tomography in the diagnosis and management of renal trauma. *Radiol Med.* 2010;115:936–49.
21. Alonso RC, Nacenta SB, Martinez PD, Guerrero AS, Fuentes CG. Kidney in danger: CT findings of blunt and penetrating renal trauma. *Radiographics.* 2009;29:2033–53.
22. Cass AS, Luxenberg M. Features of 164 bladder ruptures. *J Urol.* 1987;138:743–5.
23. Morgan DE, Nallamala LK, Kenney PJ, Mayo MS, Rue 3rd LW. CT cystography: radiographic and clinical predictors of bladder rupture. *AJR Am J Roentgenol.* 2000;174:89–95.
24. Tonkin JB, Tisdale BE, Jordan GH. Assessment and initial management of urologic trauma. *Med Clin North Am.* 2011;95:245–51.
25. Wirth GJ, Peter R, Poletti PA, Iselin CE. Advances in the management of blunt traumatic bladder rupture: experience with 36 cases. *BJU Int.* 2010;106:1344–9.
26. Koraitim MM, Marzouk ME, Atta MA, Orabi SS. Risk factors and mechanism of urethral injury in pelvic fractures. *Br J Urol.* 1996;77:876–80.
27. Ali M, Safriel Y, Sclafani SJ, Schulze R. CT signs of urethral injury. *Radiographics.* 2003;23:951–63; discussion 963–6.
28. Ingram MD, Watson SG, Skippage PL, Patel U. Urethral injuries after pelvic trauma: evaluation with urethrography. *Radiographics.* 2008;28:1631–43.
29. Ramchandani P, Buckler PM. Imaging of genitourinary trauma. *AJR Am J Roentgenol.* 2009;192:1514–23.
30. Donohue JH, Crass RA, Trunkey DD. The management of duodenal and other small intestinal trauma. *World J Surg.* 1985;9:904–13.
31. Lubner M, Demertzis J, Lee JY, Appleton CM, Bhalla S, Menias CO. CT evaluation of shock viscera: a pictorial review. *Emerg Radiol.* 2008;15:1–11.